

### Tetrahedral anisotropy of x-ray anomalous scattering

David H. Templeton and Lieselotte K. Templeton

Department of Chemistry, University of California, Berkeley, California 94720

(Received 7 January 1994)

Diffraction of synchrotron radiation in crystals of potassium chromate and germanium reveals a tetrahedral anisotropy of anomalous (resonant) scattering with respect to polarization and wave vectors that introduces a third-rank tensor into the intensity equations. This tensor arises from a mixed dipole-quadrupole term that vanishes for forward scattering and for centrosymmetric atoms. At resonances 13 eV below the Cr *K* edge and 7 eV above the Ge *K* edge large changes of intensities with rotation of azimuth are observed for weak and forbidden Bragg reflections in agreement with the optical model.

#### I. INTRODUCTION

The amplitude and phase for elastic scattering of x rays by an atom change with wavelength when there is photoelectric absorption. This dispersion is often expressed as real and imaginary anomalous scattering terms  $f'$  and  $if''$  that are added to the Thomson atomic scattering factor  $f_0$  (a Fourier transform of the electron density).<sup>1</sup> Usually it is assumed that  $f'$  and  $f''$  are scalar quantities and that the effect of polarization on amplitude for all atoms is a factor  $P = \mathbf{e} \cdot \mathbf{e}'$  for each combination of linear polarization vectors  $\mathbf{e}$  and  $\mathbf{e}'$  of incident and scattered rays. In some materials the anisotropy of atomic environment and chemical bonding is sufficient, for wavelengths near absorption edges, to give rise to significant dichroism, birefringence, and anisotropic anomalous scattering. All of these properties require a more complicated description with tensors to describe the effects of polarization.<sup>2-5</sup> Tensors of second rank have been sufficient in most cases until now. Here we report experiments that require a third-rank tensor, a type not used before in this context, to explain the anisotropy of scattering by Cr and Ge atoms in tetrahedral environments. This anisotropic scattering arises from a mixed dipole-quadrupole term in resonant scattering. For Cr in  $K_2CrO_4$  it is associated with an absorption line 13 eV below the main Cr *K* edge. In elemental Ge it is found at a resonance that is 7 eV above the Ge *K* edge. This resonance is not resolved from others in the absorption spectrum. In each case the tetrahedral symmetry causes the second-rank tensor effects to be isotropic and thus simplifies the search for anisotropic higher-order terms.

#### II. OPTICAL MODEL

According to second-order perturbation theory and neglecting magnetic transitions, the amplitude of anomalous scattering that is due to resonance of ground state  $a$  with excited state  $b$  is proportional to a product of matrix elements (plus a small nonresonant term of the same algebraic form) (Refs. 6 and 7)

$$A \sim \frac{\langle a | \mathbf{e}' \cdot \mathbf{r} \exp(-i\mathbf{k}' \cdot \mathbf{r}) | b \rangle \langle b | \mathbf{e} \cdot \mathbf{r} \exp(i\mathbf{k} \cdot \mathbf{r}) | a \rangle}{E_a - E_b + \hbar\omega - i\Gamma/2}, \quad (1)$$

where  $\mathbf{k}$  and  $\mathbf{k}'$  are wave vectors (with magnitude  $2\pi/\lambda$ ) of incident and scattered rays. The total atomic scattering factor  $f(\mathbf{e}, \mathbf{e}')$  is a sum of  $A$  for all resonances plus the Thomson scattering  $\mathbf{e} \cdot \mathbf{e}' f_0$ . Expansion of the exponential factors in (1) as power series

$$\exp(\pm i\mathbf{k} \cdot \mathbf{r}) = 1 \pm i\mathbf{k} \cdot \mathbf{r} - \frac{1}{2}(\mathbf{k} \cdot \mathbf{r})^2 \mp \dots \quad (2)$$

permits  $f$  to be expressed as a tensor series (summation implied by repeated indices)

$$\begin{aligned} f(\mathbf{e}, \mathbf{e}') = & \mathbf{e} \cdot \mathbf{e}' f_0 + e_m e'_n S^{mn} - ie_m e'_n (k'_p - k_p) T^{mnp} \\ & + e_m e'_n k'_p k_q U^{mnpq} \\ & - e_m e'_n (k'_p k'_q + k_p k_q) V^{mnpq} + \dots \end{aligned} \quad (3)$$

For brevity we designate the tensor terms as

$$f(\mathbf{e}, \mathbf{e}') = Pf_0 + Q_d - iQ_{dq} + Q_q - Q_{dq} + \dots \quad (4)$$

The dipole approximation, using only the first term of (2), neglects the spatial extent of the atom and gives only the first two terms in (3) and (4). This model has been used to interpret most of the experiments to date concerning polarization anisotropy of x-ray absorption and resonant scattering. Effects of higher terms have been observed in polarization dependence of absorption spectra<sup>8,9</sup> and in the angular dependence of the Borrmann effect.<sup>6</sup> The demonstration that anisotropy of tensors of higher rank gives observable effects in diffraction intensities was the discovery by Finkelstein, Shen, and Shastri<sup>10</sup> of nonmagnetic scattering for a forbidden reflection in hematite. In that experiment the symmetry of the iron atom on a threefold axis ruled out dipole effects as an explanation, and the scattering was attributed to quadrupole transitions. That result stimulated us to look for the effects reported here that correspond to the third-rank tensor term  $Q_{dq}$  in (4). This mixed dipole-quadrupole term is absent in forward scattering because  $\mathbf{k}' = \mathbf{k}$ . It also vanishes by symmetry if the atom is centrosymmetric, as in the models that have been used in most theoretical calculations of x-ray dispersion.

Neglecting tensors of rank higher than four, the structure factor (including polarization effects) for any crystal with  $N$  atoms per unit cell is

$$F_{\mathbf{h}} = \sum_{n=1}^N [Pf_{0n} + Q_{dn} - iQ_{dq} + Q_{qn} - Q_{don}] D_n \exp(i\mathbf{h} \cdot \mathbf{x}_n), \quad (5)$$

where  $D_n$  is the thermal factor and  $\mathbf{h} = \mathbf{k}' - \mathbf{k}$ . Because the tensors of even rank are invariant on inversion while  $Q_{dq}$  changes sign, for a centrosymmetric crystal (5) can be written

$$F_{\mathbf{h}} = 2 \sum_{n=1}^{N/2} D_n [(Pf_{0n} + Q_{dn} + Q_{qn} - Q_{don}) \cos(\mathbf{h} \cdot \mathbf{x}_n) + Q_{dq} \sin(\mathbf{h} \cdot \mathbf{x}_n)]. \quad (6)$$

For tetrahedral atomic symmetry the dipole term  $Q_d$  reduces to  $P(f' + if'')$ . The factors  $k'_p - k_p$  in (3) cause  $Q_{dq}$  to increase with Bragg angle, and the sine factor in (6) makes the effect of this term large when the cosine is small. Thus the anisotropy due to tetrahedral bonding is most evident in weak reflections at high angle. We have not identified effects of the fourth-rank tensors in these experiments, and they are disregarded in the following.

In a Cartesian basis with axes in the directions of twofold axes,  $T_d$  symmetry limits the tensor  $T$  to six equal nonzero complex elements

$$T^{mnp} = \delta = \delta' + i\delta'' \quad (m \neq n \text{ and } m \neq p \text{ and } n \neq p). \quad (7)$$

Reflections forbidden by glide-plane rules or by structure-factor algebra appear with intensities that are proportional to  $|\delta|^2$ . During azimuthal rotations  $Q_{dq}$  changes sign, and when it is added to a larger amplitude the modulation of counting rates is proportional to the first power of  $\delta$ . This modulation is sensitive to the complex phase of  $\delta$  and allows estimates of both  $\delta'$  and  $\delta''$ .

### III. POTASSIUM CHROMATE

Potassium chromate was chosen for the first experiments because of its suitable physical properties and symmetry and because Cr in this chemical state has an ab-

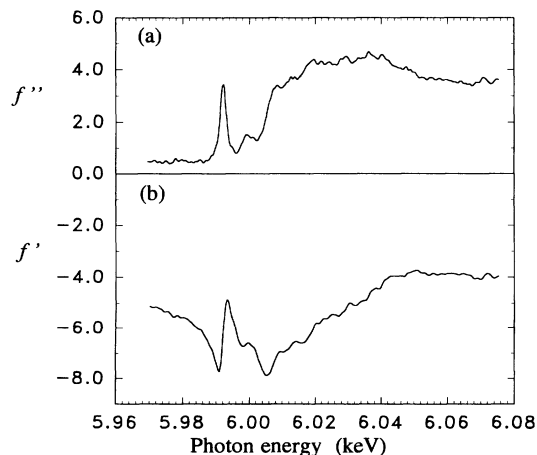


FIG. 1. Dispersion terms (a)  $f''$  and (b)  $f'$  for Cr in  $K_2CrO_4$  calculated from absorption data.

TABLE I. Dispersion parameters for chromium.

Photon energy (eV)	5991.5	5992.1	5992.7
$f'$	-9.0		-4.2
$f''$	3.2		3.2
$\delta'$ (Å)	-0.086		0.085
$\delta''$ (Å)	0.114		0.118
$ \delta $ (Å)	0.143	0.22	0.145

sorption line near its  $K$  edge that seemed likely to cause anisotropic scattering (Fig. 1). Its crystals are orthorhombic, space group  $Pnma$ , with cell dimensions  $a = 7.662$ ,  $b = 5.919$ ,  $c = 10.391$  Å.<sup>11</sup> The Cr atoms, in sites 4(c) on the mirror planes, are at centers of nearly regular tetrahedra of oxygen atoms. The four orientations of these tetrahedra differ by inversion or by reflection in one of the glide planes. Reflections ( $hk0, h$  odd) and ( $0kl, k+l$  odd) are forbidden by glide-plane rules but permitted by the anisotropic anomalous scattering.

Integrated intensities for  $\omega$  scans were measured at various wavelengths and at many settings of the azimuthal angle  $\psi$  for weak Bragg reflections in a search for some that showed anisotropy. Values of the isotropic  $f'$  and  $f''$ , the tensor parameters  $\delta'$  and  $\delta''$ , and a scale factor were determined by trial-and-error fitting of observed and calculated intensities for six reflections measured 0.6 eV above and below the center of the pre-edge absorption line (Table I). The intensities of reflections in this set were observed to change with azimuth by factors ranging from 1.1 to 3.6 (disregarding about 1% of the points

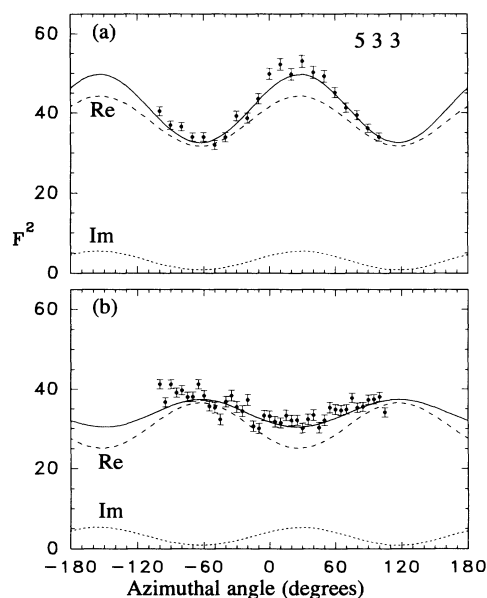


FIG. 2. Change of intensity with azimuthal angle for (533) of  $K_2CrO_4$  with photon energy 0.6 eV (a) above and (b) below the resonance peak. Solid curves are calculated using the parameters in Table I; broken curves are contributions of the real and imaginary parts of the structure factors. The change of sign of  $\delta'$  reverses the modulation of the real part.

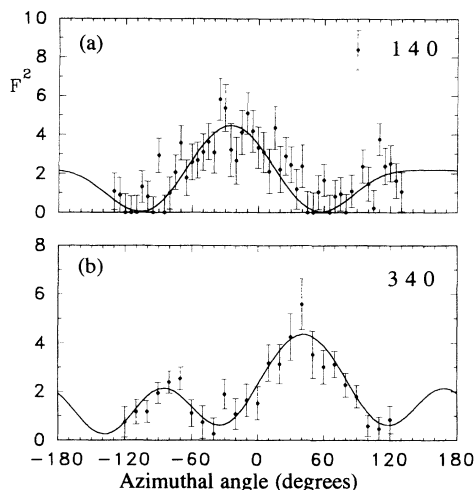


FIG. 3. Observed and calculated azimuthal variation of intensity at the resonance peak for (a) (140) and (b) (340), two reflections forbidden by a glide-plane rule in  $K_2CrO_4$ .

where the Renninger effect increased the count rate by factors up to 4). An example of the fit is shown in Fig. 2 for a reflection that shows the effect of the opposite of sign of  $\delta'$  at the two energies.

Similar measurements of glide-plane-forbidden reflections at the peak of the absorption line showed intensities that varied with azimuth in agreement with theory with  $|\delta|=0.22$  (Fig. 3). At this wavelength  $|h|$  approaches  $6.07 \text{ \AA}^{-1}$  at high Bragg angle, and thus  $Q_{dq}$  can exceed 1.3 units, an amount more than the normal scattering of an atom of lithium at the same angle.

#### IV. GERMANIUM

Germanium is cubic, space group  $Fd3m$ , with  $a=5.6577 \text{ \AA}$  at  $25^\circ\text{C}$ .<sup>12</sup> Atoms are in special positions  $8(a)$  with  $T_d$  site symmetry. Reflections  $(0kl, k+l=4n+2)$  are forbidden by the glide-plane rule.

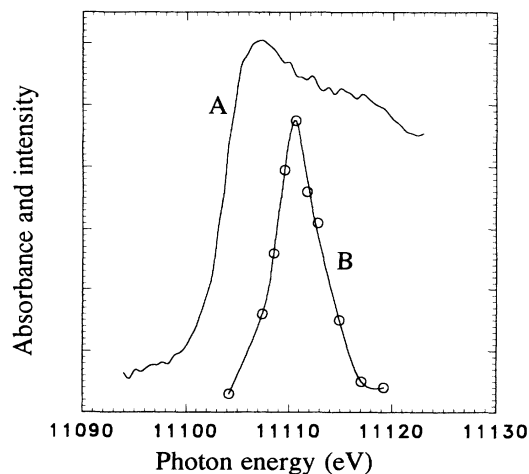


FIG. 4. Absorption spectrum of Ge at the K edge (A) and the intensity of (482) vs photon energy (B). Vertical scales are arbitrary and independent.

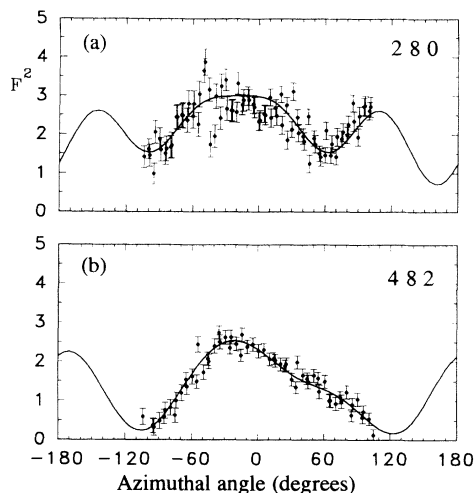


FIG. 5. Observed and calculated variation of intensity with azimuth for reflections of Ge that are forbidden (a) by a glide rule (280) and (b) by structure-factor algebra (482).

Reflections  $(hkl, h+k+l=4n+2)$  are forbidden by the special-position rule if the scattering density of each atom is centrosymmetric. Some of them at lower angles can be observed because bonding and thermal motion cause the atoms to be not quite centric.<sup>13</sup> Anisotropy of scattering allows these reflections to be observed in violation of both rules. A search for them at high Bragg angles was fruitless at and below the absorption edge, but several were found in a narrow interval of wavelength when higher energies were tested.

The intensity of (482) at  $\psi=0$  as a function of photon energy (Fig. 4) shows the location of the sharp resonance 7 eV above the K absorption edge. Integrated intensities as a function of azimuth, measured at the peak of this resonance, are shown for (280) and (482) in Fig. 5. The scale of intensity is set by comparison of observed and calculated structure factors for (800), a strong reflection measured in the same experiment. The theoretical curves in Fig. 5 correspond to  $|\delta|=0.030$ .

#### V. EXPERIMENTAL DETAILS

Diffraction data were recorded using the Enraf-Nonius CAD-4 diffractometer<sup>14</sup> on Beam Line 1-5 at SSRL (bending magnet, 50–90 mA ring current at 3 GeV, unfocused, double-crystal Si(111) monochromator) as described elsewhere.<sup>15</sup> A well-formed crystal of  $K_2CrO_4$ ,  $\sim 0.07 \times 0.2 \times 0.5 \text{ mm}$ , and an irregular plate of Ge,  $\sim 0.07 \times 0.5 \times 0.5 \text{ mm}$ , were glued to the ends of glass fibers. Typical gross count rates for a forbidden reflection in  $K_2CrO_4$  [Fig. 3(b)] were 16 c/s at the peak of a scan and 6 c/s when averaged over a scan width of  $0.13^\circ$ , with background 4 c/s. Some allowed reflections at similar Bragg angles were more than 1000 times stronger. For a forbidden reflection in Ge [Fig. 5(b)] a maximum count rate was 3000 c/s, average over a  $0.22^\circ$  scan 350 c/s, background 250 c/s. Integrated intensities were corrected for absorption by analytical integration. Wavelengths were set with a precision of about 0.2 eV (Cr) or 0.4 eV (Ge) using absorption spectra of polycrystalline

$K_2CrO_4$  or Ge, but the absolute scales are less certain. The energy bandwidth (fullwidth at half maximum) is estimated as  $\Delta E/E = 1 - 1.5 \times 10^{-4}$ . The radiation was assumed to be 91.5% linearly polarized, based on measurements at other times on this beam line. Calculated intensities contain small corrections for this imperfect polarization.

## VI. DISCUSSION

Chemical bonding of Cr or Ge to its four neighbors is associated with an increase of electron density in the bonds. In a molecular-orbital model this increase comes from occupation of bonding orbitals. We attribute the anisotropic resonances to transitions to the corresponding antibonding orbitals that are empty and that are concentrated in the tetrahedral directions opposite to the bonds. In the Cr case the signs of  $\delta'$  and  $\delta''$  (for a given choice of tensor coordinates) distinguish bond and antibond directions and confirm the antibond direction as the location of maximum overlap of the wave functions in (1). The maximum magnitude of  $\delta$  at each resonance is the product of an oscillator strength and an effective distance from the atomic nucleus. The effective distances for overlap of the  $1s$  core level with valence-band orbitals are expected to be of the same order of magnitude as those for  $1s$  with  $4p$  hydrogenic wave functions, estimated by numerical integration as  $0.07 \text{ \AA}$  for Cr and  $0.06 \text{ \AA}$  for Ge. On this basis we estimate oscillator strengths for the resonances to be about 3 and 0.5 for Cr and Ge, respectively. This value for Cr is the same as that derived from the absorption data for the isotropic dipole term (Fig. 1). In Ge the antibonding states lie among other empty states, and the oscillator strength is small enough to avoid prominence in the absorption spectrum (Fig. 4).

Because the energy resolution of the experiments is comparable to the level widths, we expect that higher values would be found for  $\delta$  (and for the dispersion at the Cr absorption line) in measurements with more nearly monochromatic radiation.

Tetrahedral bonding is widespread in chemistry, and these results greatly expand the domain of materials in which anisotropic dispersion can be studied or applied. The Ge experiment shows how this new technique can reveal a level that is not seen with simpler spectroscopy. Since  $Q_{dq}$  is proportional to  $\sin\theta$ , the measurement of this tensor term is perhaps the most direct demonstration yet that dispersion changes with Bragg angle and that the change is too large to be disregarded in diffraction experiments near absorption edges.

## ACKNOWLEDGMENTS

We thank the many staff members of Stanford Synchrotron Radiation Laboratory whose assistance made this work possible. We are particularly indebted to Dr. Michael Soltis. This research was supported in its initial stages by the National Science Foundation under Grant No. CHE-8821318. It was done in part at SSRL, which is operated by the Department of Energy, Office of Basic Energy Sciences. The SSRL Biotechnology Program is supported by the NIH, Biomedical Resource Technology Program, Division of Research Resources. Further support is provided by the Department of Energy, Office of Health and Environmental Research. Also used were facilities of the Lawrence Berkeley Laboratory, supported by the Director, Office of Energy Research, Office of Basic Energy Sciences, Chemical Sciences Division of the US Department of Energy under Contract No. DE-AC03-76SF00098.

<sup>1</sup>R. W. James, *The Optical Principles of the Diffraction of X-Rays* (Ox Bow, Woodbridge, 1982).

<sup>2</sup>D. H. Templeton and L. K. Templeton, *Acta Crystallogr. A* **38**, 62 (1982); **44**, 1045 (1988).

<sup>3</sup>V. E. Dmitrienko, *Acta Crystallogr. A* **39**, 29 (1983).

<sup>4</sup>V. A. Belyakov and V. E. Dmitrienko, *Usp. Fiz. Nauk* **158**, 679 (1989) [*Sov. Phys. Usp.* **32**, 697 (1989)].

<sup>5</sup>C. Brouder, *J. Phys. Condens. Matter* **2**, 701 (1990).

<sup>6</sup>H. Wagenfeld, *Phys. Rev.* **144**, 216 (1966).

<sup>7</sup>M. Blume, *J. Appl. Phys.* **57**, 3615 (1985).

<sup>8</sup>J. E. Hahn, R. A. Scott, K. O. Hodgson, S. Doniach, S. R. Desjardins, and E. I. Solomon, *Chem. Phys. Lett.* **88**, 595 (1982).

<sup>9</sup>G. Dräger, R. Frahm, G. Materlik, and O. Brümmer, *Phys. Status Solidi B* **146**, 287 (1988).

<sup>10</sup>K. D. Finkelstein, Q. Shen, and S. Shastri, *Phys. Rev. Lett.* **69**, 1612 (1992).

<sup>11</sup>K. Toriumi and Y. Saito, *Acta Crystallogr. B* **34**, 3149 (1978).

<sup>12</sup>M. E. Straumanis and E. Z. Aka, *J. Appl. Phys.* **23**, 330 (1952).

<sup>13</sup>B. Dawson, *Proc. R. Soc. London, Ser. A* **298**, 255 (1967).

<sup>14</sup>J. C. Phillips, J. A. Cerino, and K. O. Hodgson, *J. Appl. Crystallogr.* **12**, 592 (1979).

<sup>15</sup>D. H. Templeton and L. K. Templeton, *Acta Crystallogr. A* **42**, 478 (1986).